J|A|C|S ARTICLES

Published on Web 07/16/2009

Kinetic Hydrogen/Deuterium Effects in the Direct Hydrogenation of Ketones Catalyzed by a Well-Defined Ruthenium Diphosphine Diamine Complex

Marco Zimmer-De Iuliis and Robert H. Morris*

Davenport Laboratory, Department of Chemistry, University of Toronto, Toronto, Ontario M5S 3H6, Canada

Received May 28, 2009; E-mail: rmorris@chem.utoronto.ca

Abstract: The *trans*-dihydride complex *trans*-$RuH_2(NH_2CMe_2CMe_2NH_2)$((*R*)-binap) (**1**) is an active catalyst for the homogeneous hydrogenation of ketones in benzene under pressure of H_2 gas. The mechanism of the catalysis is proposed to occur through a rapid transfer of a hydride from the ruthenium and a proton from the amine on **1** to the carbonyl of the ketone to give the product alcohol and a hydrido-amido intermediate $RuH(NHCMe_2CMe_2NH_2)$((*R*)-binap) (**2**). The dihydride is then regenerated by the turnover-limiting heterolytic splitting of dihydrogen by complex **2**. In this work the kinetic isotope effect (KIE) is measured to be 2.0 (±0.1) for the reduction of acetophenone to 1-phenylethanol catalyzed by **1** using 8.0 atm of H_2 versus D_2 gas. DFT calculations predict a KIE of 2.1 for the described mechanism using the simplified catalyst $RuH(NHCH_2CH_2NH_2)(PH_3)_2$ with H_2 or the catalyst $RuD(NDCH_2CH_2ND_2)(PH_3)_2$ with D_2. This supports the observation that deuterium scrambles into the catalyst when a pressure of D_2 is used. We discuss the significance of these results relative to the KIE of 2 that was reported by Sandoval et al. (*J. Am. Chem. Soc.* **2003** *125*, 13490) for the hydrogenation/deuteriation of acetophenone catalyzed by *trans*-$RuH(\eta^1\text{-}BH_4)$((*S*)-tolbinap)((*S,S*)-dpen) in basic isopropanol/isopropanol-d_8.

Introduction

The substitution of deuterium for hydrogen is a useful technique in the study of the mechanism of catalytic hydrogenation reactions. Labeling the gas,[1−16] the substrate,[17−19] the catalyst,[20,21] or the solvent[7,22−24] with deuterium is practical and has yielded important mechanistic insights.

The measurement of kinetic isotope effects for catalytic processes by use of dihydrogen and dideuterium is less common. Noyori and co-workers measured the kinetic isotope effect (KIE) of the asymmetric hydrogenation (or deuteriation) of acetophenone catalyzed by *trans*-$RuH(\eta^1\text{-}BH_4)$((*S*)-tolbinap)((*S,S*)-dpen) in isopropanol or isopropanol-d_8 (Table 1).[25] They found a large variability in the value. Under highly basic conditions (KOtBu/catalyst = 200/1), a value of 2 was reported, while in the absence of added KOtBu, a large value of 55 was reported. The small value was proposed to result from the rate-determining splitting of dihydrogen across a ruthenium−amido bond (structure I, Figure 1)[25−29] or by a proton shuttle involving the alcohol solvent (structure II, Figure 1).[25] The large value was proposed to result from the rate-limiting deprotonation of a cationic dihydrogen complex by the alcohol solvent (B) (Figure 1, structure III) although recent work by Hamilton and Bergens suggests that such a dihydrogen complex is not found within the catalytic cycle.[22,30]

(1) Smith, G. V.; Musoiu, M. *J. Catal.* **1979**, *60*, 184–192.
(2) Brown, J. M.; Parker, D. *Organometallics* **1982**, *1*, 950–956.
(3) Willoughby, C. A.; Buchwald, S. L. *J. Am. Chem. Soc.* **1994**, *116*, 11703–11714.
(4) Hardick, D. J.; Blagbrough, I. S. *J. Am. Chem. Soc.* **1996**, *118*, 5897–5903.
(5) Kimmich, B. F. M.; Somsook, E.; Landis, C. R. *J. Am. Chem. Soc.* **1998**, *120*, 10115–10125.
(6) Aime, S.; Canet, D.; Dastru, W.; Gobetto, R.; Reineri, F.; Viale, A. *J. Phys. Chem. A* **2001**, *105*, 6305–6310.
(7) Ito, M.; Hirakawa, M.; Murata, K.; Ikariya, T. *Organometallics* **2001**, *20*, 379–381.
(8) Berkessel, A.; Schubert, T. J. S.; Müller, T. N. *J. Am. Chem. Soc.* **2002**, *124*, 8693–8698.
(9) Lange, S.; Leitner, W. *J. Chem. Soc., Dalton Trans.* **2002**, *16*, 752–758.
(10) Solladie-Cavallo, A.; Hoernel, F.; Schmitt, M.; Garin, F. *J. Mol. Cat. A* **2003**, *195*, 181–188.
(11) Dahlenburg, L.; Gotz, R. *Eur. J. Inorg. Chem.* **2004**, *31*, 888–905.
(12) Lin, S. T.; Siegel, S. *Kinet. Katal.* **2006**, *47*, 83–92.
(13) Yoshimura, M.; Ishibashi, Y.; Miyata, K.; Bessho, Y.; Tsukamoto, M.; Kitamura, M. *Tetrahedron* **2007**, *63*, 11399–11409.
(14) Legault, C. Y.; Charette, A. B.; Cozzi, P. G. *Heterocycles* **2008**, *76*, 1271–1283.
(15) Zuidema, E.; Escorihuela, L.; Eichelsheim, T.; Carbo, J. J.; Bo, C.; Kamer, P. C. J.; Van Leeuwen, P. W. N. *Chem.−Eur. J.* **2008**, *14*, 1843–1853.
(16) Heiden, Z. M.; Rauchfuss, T. B. *J. Am. Chem. Soc.* **2009**, *131*, 3593–3600.
(17) Pàmies, O.; Bäckvall, J.-E. *Chem.−Eur. J.* **2001**, *7*, 5052–5058.
(18) Zhao, J.; Hesslink, H.; Hartwig, J. F. *J. Am. Chem. Soc.* **2001**, *123*, 7220–7227.
(19) Bäckvall, J.-E. *J. Organomet. Chem.* **2002**, *652*, 105–111.
(20) Casey, C. P.; Johnson, J. B. *J. Am. Chem. Soc.* **2005**, *127*, 1883–1894.
(21) Ralph, C. K.; Hamilton, R. J.; Bergens, S. H. In *The Handbook of Homogeneous Hydrogenation*; de Vries, J. G., Elsevier, C. J., Eds.; Wiley-VCH: New York, 2007; Vol. 1, pp 359−371.
(22) Hamilton, R. J.; Bergens, S. H. *J. Am. Chem. Soc.* **2006**, *128*, 13700–13701.
(23) Kamitanaka, T.; Matsuda, T.; Harada, T. *Tetrahedron* **2007**, *63*, 1429–1434.
(24) Starodubtseva, E. V.; Turova, O. V.; Vinogradov, M. G.; Gorshkova, L. S.; Ferapontov, V. A. *Russ. Chem. Bull.* **2007**, *56*, 552–554.

Table 1. Kinetic Isotope Effects for Reactions of Dihydrogen Versus Dideuterium

reaction	RDS[a]	$k(H_2)/k(D_2)$	ref
H_2 + PhCOMe + *trans*-RuH(η^1-BH_4)((*S*)-tolbinap)((*S,S*)dpen) + KOtBu	H_2 + N−Ru^{II}, TS I of Figure 1 or H_2 + N−Ru^{II} + ROH, TS II	2[b]	25
H_2 + PhCOMe + *trans*-RuH(η^1-BH_4)((*S*)-tolbinap)((*S,S*)-dpen)	H_2 + HN−Ru^{II}	55[c]	25
H_2 + *trans*-IrCl(CO)(PPh_3)$_2$	H_2 + Ir^I	1.22	31
H_2 + (*Z*)-PhHC═C(NHCOMe)(COOH) + $[Rh(PPh_2CH_2CH_2PPh_2)(MeOH)_2]^+$	H_2 + Rh^I	1.23 ± 0.05	2
H_2 + (Z)-R-(acetamido)cinnamate + Ru$(OAc)_2$((*R*)-binap)	H_2 + C−Ru^{II}	1.2	40
H_2 + 2-phenylpyrroline catalyzed by a chiral titanocene complex	H_2 + N−Ti^{IV}	1.5	3

[a] Rate determining step. [b] iPrOH solvent and KOtBu. [c] iPrOH solvent without base.

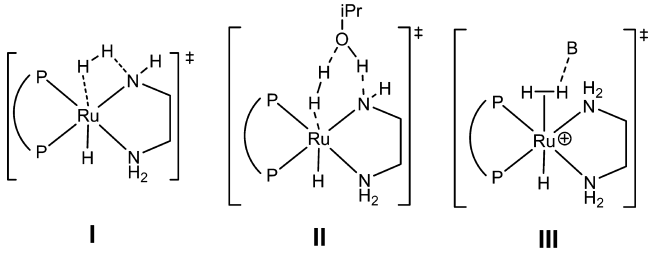

Figure 1. Three transition states proposed by Noyori and co-workers (ref 25) for the formation of the *trans*-dihydride in the presence of added KOtBu (**I** or **II**) and in the absence of added KOtBu (**III**) where the base is proposed to be the alcohol solvent. P−P is (*S*)-tolbinap and the diamine is (*S,S*)-dpen.

Other relevant kinetic isotope effect (KIE) values are listed in Table 1. In 1966 Chock and Halpern reported a KIE of 1.22 for the oxidative addition of H_2/D_2 to *trans*-IrCl(CO)$(PPh_3)_2$.[31] This and other data provided evidence for a side-on interacting dihydrogen in the transition state.[32,33] Zhou et al. used empirical methods to estimate the relative importance of tunneling, zero-point energy, vibrational, translational and rotational partition functions that make up this small KIE value.[34] Significantly, Brown and Parker found that the KIE for the hydrogenation of (*Z*)-acetamidocinnamic acid catalyzed by $[Rh(dppe)(OHMe)_2]^+$ in methanol is identical at 1.23 ± 0.05.[2] Landis and co-workers proposed that this value, on the basis of DFT calculations, results from the combined isotope effects of three steps, first the addition of dihydrogen to rhodium(I) to give a dihydrogen complex in a rapid equilibrium step (with an inverse equilibrium isotope effect (EIE) of 0.8) followed by oxidative addition in a second equilibrium step to give a rhodium(III) dihydride (inverse EIE of 0.8) followed by a slow migratory-insertion of the olefin into the rhodium-hydride bond (KIE of 1.8), giving an overall KIE of 1.15.[35] The source of the inverse equilibrium isotope effect (0.65−0.8) for H_2 coordination has been explained for iridium complexes[36,37] and chromium group complexes.[38] Parkin has reviewed EIE values for a variety of other reactions.[39] The turnover-limiting hydrogenolysis of a ruthenium−alkyl bond was proposed for the hydrogenation of methyl (*Z*)-(*R*)-(acetamido)cinnamate catalyzed by Ru$(OAc)_2$((*R*)-binap), and this was supported by a KIE of 1.2.[40] In the hydrogenation of the imine 2-phenylpyrroline catalyzed by a chiral titanocene complex, a KIE of 1.5 ± 0.2 was attributed to the turnover-limiting hydrogenolysis of a titanium−amido bond.[3] The theoretical maximum isotope effect for the gases themselves, neglecting tunneling, is 20 where the H−H bond versus the D−D bond is completely broken in the transition state.[41]

Our research group had previously demonstrated that the heterolytic splitting of dihydrogen is the turnover-limiting step in the catalytic hydrogenation of acetophenone using *trans*-$RuH_2(NH_2CMe_2CMe_2NH_2)$((*R*)-binap) (**1**) in benzene in the absence of added base.[27,28] Here we both measure and calculate the kinetic isotope effect for this well-defined catalyst system. To the best of our knowledge the current report is the first to calculate by use of DFT the isotope effects for the catalytic H_2-hydrogenation of ketones based on ruthenium phosphine/diamine systems and a rare example where the results of both experiment and theory of the KIE for catalytic hydrogenation are compared. While dihydrogen splitting is turnover-limiting in our system, in a related study Comas-Vives et al.[42a] utilized DFT methods to calculate the isotope effects for the transfer of hydrogen or deuterium from a Shvo-type ruthenium catalyst to formaldehyde. They found that the concerted outer-sphere transfer transition state that was proposed by Casey and co-workers[42b] was most consistent with the calculated and experimentally observed KIE.[42c]

Experimental Details

General. Unless otherwise stated, all manipulations were carried out under Ar using standard Schlenk and glovebox techniques. The literature method for the preparation of RuH_2(tmen)((*R*)-binap),[27,28] where tmen is $NH_2CMe_2CMe_2NH_2$, was modified to provide a better yield (see below). All of the solvents were distilled under argon

(25) Sandoval, C. A.; Ohkuma, T.; Muñiz, K.; Noyori, R. *J. Am. Chem. Soc.* **2003**, *125*, 13490–13503.
(26) Abdur-Rashid, K.; Lough, A. J.; Morris, R. H. *Organometallics* **2000**, *19*, 2655–2657.
(27) Abdur-Rashid, K.; Faatz, M.; Lough, A. J.; Morris, R. H. *J. Am. Chem. Soc.* **2001**, *123*, 7473–7474.
(28) Abdur-Rashid, K.; Clapham, S. E.; Hadzovic, A.; Harvey, J. N.; Lough, A. J.; Morris, R. H. *J. Am. Chem. Soc.* **2002**, *124*, 15104–15118.
(29) Noyori, R.; Ohkuma, T. *Angew. Chem., Int. Ed.* **2001**, *40*, 40–73.
(30) Hamilton, R. J.; Leong, C. G.; Bigam, G.; Miskolzie, M.; Bergens, S. H. *J. Am. Chem. Soc.* **2005**, *127*, 4152–4153.
(31) Chock, P. B.; Halpern, J. *J. Am. Chem. Soc.* **1966**, *88*, 3511.
(32) Halpern, J. *Acc. Chem. Res.* **1970**, *3*, 386–392.
(33) Hyde, E. M.; Shaw, B. L. *J. Chem. Soc., Dalton Trans.* **1975**, 765–767.
(34) Zhou, P.; Vitale, A. A.; San Filippo, J., Jr.; Saunders, W. H., Jr. *J. Am. Chem. Soc.* **1985**, *107*, 8049–8054.
(35) Landis, C. R.; Hilfenhaus, P.; Feldgus, S. *J. Am. Chem. Soc.* **1999**, *121*, 8741–8754.
(36) Abu-Hasanayn, F.; Krogh-Jespersen, K.; Goldman, A. S. *J. Phys. Chem.* **1993**, *97*, 5890–5896.
(37) Abu-Hasanayn, F.; Krogh-Jespersen, K.; Goldman, A. S. *J. Am. Chem. Soc.* **1993**, *115*, 8019–8023.
(38) Bender, B. R.; Kubas, G. J.; Jones, L. H.; Swanson, B. I.; Eckert, J.; Capps, K. B.; Hoff, C. D. *J. Am. Chem. Soc.* **1997**, *119*, 9179–9190.
(39) Parkin, G. J. *Labelled Compd. Radiopharm.* **2007**, *50*, 1088–1114.
(40) Kitamura, M.; Tsukamoto, M.; Bessho, Y.; Yoshimura, M.; Kobs, U.; Widhalm, M.; Noyori, R. *J. Am. Chem. Soc.* **2002**, *124*, 6649–6667.
(41) Johnson, H. S. *Gas Phase Reaction Rate Theory*; The Ronald Press Company: New York, 1966.
(42) (a) Comas-Vives, A.; Ujaque, G.; Lledós, A. *Organometallics* **2007**, *26*, 4135–4144. (b) Casey, C. P.; Bikzhanova, G. A.; Cui, Q.; Guzei, I. A. *J. Am. Chem. Soc.* **2005**, *127*, 14062–14071. (c) Casey, C. P.; Singer, S. W.; Powell, D. R.; Hayashi, R. K.; Kavana, M. *J. Am. Chem. Soc.* **2001**, *123*, 1090–1100.

using sodium/benzophenone ketyl. Acetophenone was purchased from Aldrich and distilled under argon and dried over P_2O_5. D_2 (99.8% D) gas was purchased from Cambridge Isotope Laboratories. Chromatography was carried out on a Perkin-Elmer Autosystem XL with Chrompack capillary column (Chirasil-Dex CB 25 m × 0.25 mm) utilizing an H_2 carrier gas at a column pressure of 5 psi, an oven temperature of 130 °C, an injector temperature of 250 °C, and an FID temperature of 275 °C. The retention times were 5.0 min for acetophenone, 8.4 min for (*R*)-1-phenylethanol, and 9.1 min for (*S*)-1-phenylethanol.

***trans*-RuH$_2$((*R*)-binap)(tmen) (1).** A 50 mL Schlenk flask was charged with 150 mg (0.17 mmol) of RuHCl((*R*)-binap)(tmen), 172 mg of KHB(*sec*-Bu)$_3$ (1.0 M solution in THF, 0.19 mmol) and 1 mL of THF, yielding a dark-red solution. The mixture was stirred under 1 atm of H_2 for 3 h and then filtered over a pad of Celite. Pentane (8 mL) was added to the filtrate, and the mixture was stirred under H_2 for 3−4 h, after which time an orange-red precipitate formed in the light-orange solution. The bright-orange solid was filtered, washed twice with 1 mL of pentane, and then dried for 10 min under vacuum. Yield: 108 mg, 76%. ^{1}H NMR (C_6D_6) δ: −4.80 (t, $^2J_{HP}$ = 17.2 Hz, 2H, RuH), 0.22 (s, 6H, Me), 1.00 (s, 6H, Me), 0.90 (d, $^2J_{HH}$ = 10.2 Hz, 2H, NH) 3.11 (d, $^2J_{HH}$ = 10.0 Hz, 2H, NH), 6.50−8.75 (m, 32H). ^{31}P{^{1}H} (C_6D_6) δ: 89.6 (s). These values agree well with previously reported values.[27]

Kinetics. All of the hydrogenation reactions were carried out at constant pressures of H_2 or D_2 using a stainless steel 50 mL Parr hydrogenation reactor with a glass liner. The reactor was modified such that in one of the ports a stainless steel sampling tube was added. Please see the Supporting Information for further details regarding the modifications to the reactor and the method of sampling used. The reactor was degassed by evacuation for 15 min, followed by refilling with 8.0 atm of H_2 or D_2 gas, and this was repeated three times. Standard solutions of acetophenone (0.833 M) and RuH$_2$(tmen)((*R*)-binap) (2.28×10^{-3} M) were prepared by dissolving the appropriate amount of compound in 10 mL of C_6H_6. Reaction mixtures were prepared by pipetting the appropriate amount of substrate stock solution into a 3 mL volumetric flask and catalyst stock solution into a 2 mL volumetric flask and diluting with C_6H_6, to give a total volume of 5 mL upon mixing. Substrate and catalyst solutions were taken up via separate syringes and then injected into the reactor against a flow of gas. Samples were taken every two minutes. Concentrations of 1-phenylethanol were determined via gas chromatography.

Computational Details

General. All calculations were performed using Gaussian03.[43] Calculations used the mPW1PW91 density functional method.[44,45] Ruthenium was treated with the SDD[46] basis set to include relativistic effects and an effective core potential, and H, C, N, and P were treated with the triple-ζ basis set 6-311++G** which includes diffuse functionals and additional p-orbitals on H as well as additional d-orbitals on C, N, O, and P. It has been previously demonstrated that this combination of functional is superior to the B3LYP functional and other ECP.[47,48] In addition, Lynch et al. have reported that the mPW1PW91 functional is better for the prediction of transition states and energy barriers.[49] All structures were optimized in the gas phase. Full vibrational analyses were performed on the optimized structure to obtain values of ΔG, ΔH, and ΔS at 1 atm and 298 K. The QST2 or QST3 method was utilized to locate transition states. All transition states were found to have one imaginary frequency. The calculated Atomic Polar Tensor (APT) charges were used. The APT charge is the derivative of the forces on the atoms with respect to an applied external electric field and yield atomic charges that more accurately reflect the charge distribution rather than individual atomic charges.[50] Owing to the large size of **1** and **2**, (*R*)-binap was modeled as two *cis*-PH_3 groups, and 2,3-dimethyl-2,3-diaminobutane was simplified to ethylene diamine (Figure 2). In order to calculate the isotope effect, the keyword "ISO=2" was added next to the required protons in the input file and then a full optimization and vibrational analysis was performed again to determine the free energy of the deuterated model species.

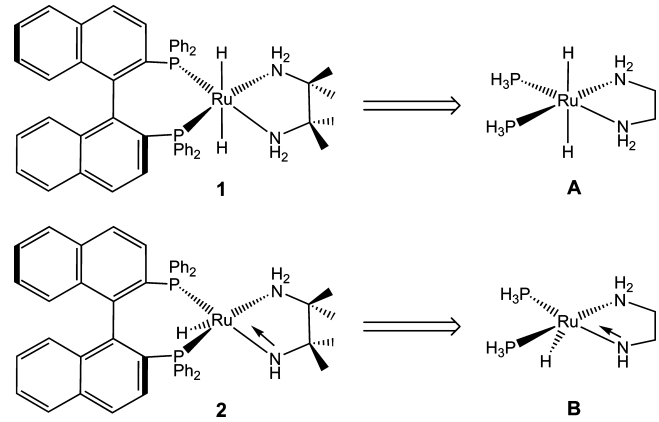

Figure 2. Simplification made for **1** and **2** for the calculation of the structures shown in Scheme 1.

Predicting the Kinetic Isotope Effect. Kinetic isotope effects (KIE) were calculated using conventional transition state theory (TST). For the reaction in which reactant, R, goes to the transition state, TS, we may write the following equations.[51,52]

$$R^H \xrightarrow{k_H} TS^H,\ k_H = \frac{k_B T}{h} \exp(-\Delta G_H^{\circ\ddagger}/RT) \quad (1)$$

$$R^D \xrightarrow{k_D} TS^D,\ k_D = \frac{k_B T}{h} \exp(-\Delta G_D^{\circ\ddagger}/RT) \quad (2)$$

In eq 1, k_H, R^H and TS^H are the rate constant, reactant and transition state for the protio species, respectively. The analogous equations when D_2 is used are shown in eq 2. $\Delta G_H^{\circ\ddagger}$ and $\Delta G_D^{\circ\ddagger}$ are respectively the activation barriers for the protio and deutero species at a given temperature T, h is Planck's constant and k_B is Boltzmann's constant. If eqs 1 and 2 are combined, then we can express the KIE as the ratio of k_H/k_D as shown below.

$$\mathrm{KIE} = \frac{k_H}{k_D} = \exp((\Delta G_D^{\circ\ddagger} - \Delta G_H^{\circ\ddagger})/RT) \quad (3)$$

It should be noted that the conventional TST adopted in the current study assumes that the geometry of the protio and deutero TS in the proposed reaction mechanisms stays the same. Also, tunneling and recrossing effects have not been accounted for since such a treatment is beyond the scope of the present study.

Results and Discussion

The new sampling method and reactor charging method allowed the economical use of deuterium gas so that the kinetics

(43) Frisch, M. J.; et al. *Gaussian 03*, Revision C.02 ed; Gaussian Inc.: Wallingford, CT, 2004.
(44) Adamo, C.; Barone, V. *J. Chem. Phys.* **1998**, *108*, 664–675.
(45) Burke, K.; Perdew, J. P.; Wang, Y. *Electronic Density Functional Theory: Recent Progress and New Directions*; Plenum: New York, 1997.
(46) Leininger, T.; Nicklass, A.; Stoll, H.; Dolg, M.; Schwerdtfeger, P. *J. Chem. Phys.* **1996**, *105*, 1052–1059.
(47) Gusev, D. G. *J. Am. Chem. Soc.* **2004**, *126*, 14249–14257.
(48) Zhang, Y.; Guo, Z.; You, X.-Z. *J. Am. Chem. Soc.* **2001**, *123*, 9378–9387.
(49) Lynch, B. J.; Truhlar, D. G. *J. Phys. Chem. A* **2001**, *105*, 2936–2941.
(50) Cioslowski, J. *J. Am. Chem. Soc.* **1989**, *111*, 8333–8336.
(51) Laidler, K. J. *Chemical Kinetics*, 3rd ed.; Harper & Row: New York, 1987.
(52) Truhlar, D. G.; Garrett, B. C. *J. Am. Chem. Soc.* **1989**, *111*, 1232.

Table 2. Kinetic Data Determined for Complex **1**[a]

gas	[Ru], M	$P(H_2$ or $D_2)$, atm; [H_2 or D_2], M	v_0, M s^{-1}	$k = v_0/$[Ru]/[H_2 or D_2], M^{-1} s^{-1}
H_2	4.6×10^{-4}	8.0; 2.1×10^{-2}	$2.4\ (\pm0.1) \times 10^{-5}$	2.5 (±0.1)
D_2	4.6×10^{-4}	8.0; 2.3×10^{-2} [b]	$1.32\ (\pm0.05) \times 10^{-5}$	1.25 (±0.05)

[a] 293 °C, benzene, 0.166 M acetophenone. [b] The solubility of D_2 is about 1.09 times greater than that of H_2.[53]

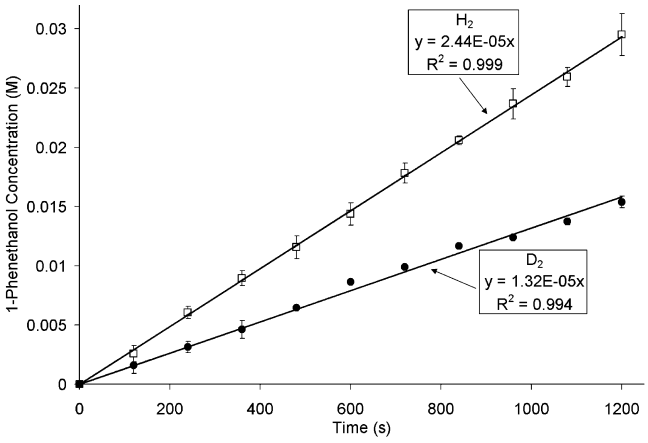

Figure 3. Plot of the average concentration of 1-phenylethanol determined using **1** with H_2 and D_2. The data points represent the average of results of four experiments for the H_2 line (gray squares) and, three experiments for the D_2 line (black circles).

Scheme 1. Mechanism for the Heterolytic Splitting of Dihydrogen, Starting with **B** and the Outer-sphere Hydrogenation of Acetone[a]

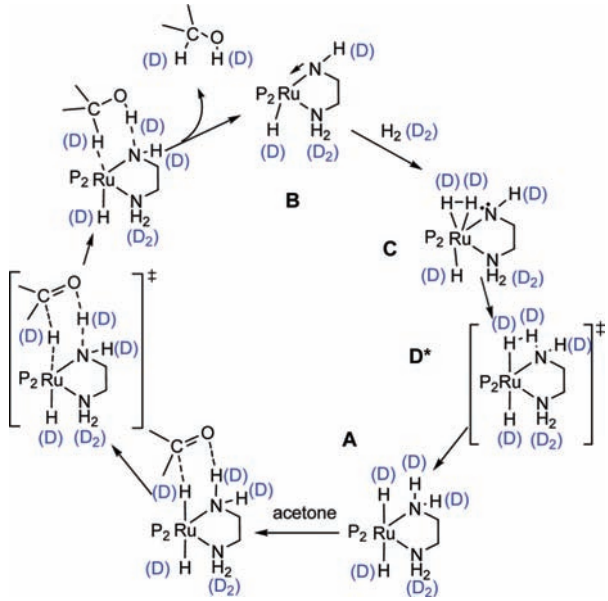

[a] $P_2 = (PH_3)_2$.

of the reactions shown in eq 4 could be made at 8 atm pressure, 20 °C. The results are shown in Table 2 and Figure 3.

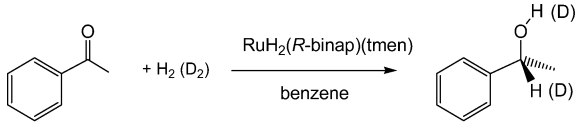

(4)

The rate constant for H_2 is 2.5 ± 0.1 M^{-1} s^{-1} which is slightly lower than that of the literature value of 3.6 M^{-1} s^{-1}.[28] The rate constant using D_2 under the same conditions is 1.32 ± 0.05 M^{-1} s^{-1} taking into account the slightly higher solubility of D_2 than that of H_2 in benzene. Therefore, the kinetic isotope effect is 2.0 ± 0.1. The magnitude of this isotope effect is indicative of an early transition state in which there is only a little weakening of the H−H bond.

The mechanism of hydrogenation using **1** has been proposed to occur as shown in Scheme 1.[27,28] As the catalysis proceeds using D_2 gas, eventually all of the N−H protons and the Ru−H hydrides will be replaced with deuterium according to this mechanism. The time for the replacement of these hydrogens for deuteria can be estimated from the turnover frequency of the reaction with D_2 gas of 0.028 s^{-1} (1.32×10^{-5} M s^{-1}/4.6×10^{-4} M) or 36 s per turnover. After the first addition of D_2 to **2** to give *trans*-RuD(H)((*R*)-binap)($NDHCMe_2CMe_2NH_2$), D_2 can be added to a ketone from the side of the molecule containing the DRuND unit, or H_2 can be added from the HRuNH unit on the other side of the otherwise C_2-symmetrical *trans*-dihydride (ignoring the H vs D distinction when determining the symmetry). The HRuNH transfer should be faster so that after less than 16 cycles of 36 s (480 s), the catalyst will be in the form *trans*-RuD_2((*R*)-binap)($ND_2CMe_2CMe_2ND_2$). The rapid deuteration of **1** in toluene under D_2 gas has been reported previously.[27] Therefore, complete deuteration in these positions of the catalyst actually takes place much earlier than 480 s. Thus, the deuteration of the catalyst must be taken into account when calculating the kinetic isotope effect for the catalytic process by use of the DFT method (see below).

Often alcohols are the best solvents for the hydrogenation of ketones catalyzed by ruthenium complexes containing primary amines and phosphines.[7,29,54,55] In one case our group showed that, as alcohol is produced in the hydrogenation of acetophenone catalyzed by RuH($NHCMe_2py$)(((*R*)-binap) in benzene, the reaction speeds up in an autocatalytic fashion.[56] An explanation for all of these observations is a proton-shuttle transition state analogous to **II** shown in Figure 1. Calculations have shown that this six-membered transition state has a lower barrier to dihydrogen splitting than the four-membered one analogous to **I**.[56,57] However, the rate of the hydrogenation of acetophenone catalyzed by **1** remains constant as the 1-phenylethanol concentration increases (Figure 3)[28] so that an alcohol-assisted splitting of dihydrogen is not operative in this case. The bulkier diamine of **1** might destabilize the hydrogen-bonded network required for the transition state **II** of Figure 1.

Another possible complication in understanding the mechanism of the hydrogenation of acetophenone catalyzed by **1** is the formation of the alkoxide complex *trans*-RuH(OCHMePh)(binap)(tmen) by the known, reversible reaction of 1-phenylethanol with the amido complex **2**.[28] This reaction does not appear to be important under the catalytic conditions of low concentrations of catalyst and substrate utilized in this work. In addition the 1-phenylethanol is very weakly acidic in benzene, a low dielectric solvent, disfavoring the protonation of the amido complex to give a cationic complex that might lead to the formation of a transition state like **III** of Figure 1. The work of

(53) Muccitelli, J.; Yen, W.-Y. *J. Soln. Chem.* **1978**, *7*, 257.
(54) Rautenstrauch, V.; Hoang-Cong, X.; Churlaud, R.; Abdur-Rashid, K.; Morris, R. H. *Chem.—Eur. J.* **2003**, *9*, 4954–4967.
(55) Genov, D. G.; Ager, D. J. *Angew. Chem., Int. Ed.* **2004**, *43*, 2816–2819.
(56) Hadzovic, A.; MacLaughlin, C. M.; Song, D.; Morris, R. H. *Organometallics* **2007**, *26*, 5987–5999.

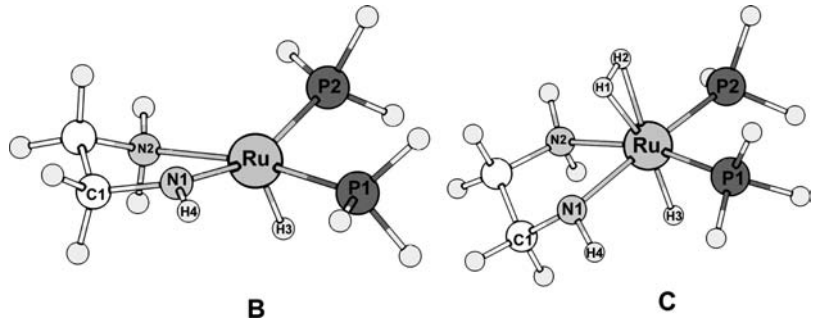

Figure 4. Calculated structures of models **B** and **C**.

Hamilton and Bergens[22,58] shows that, when isopropanol is the solvent, the alkoxide complexes *trans*-RuH(OR)(binap)(dpen) are the resting states for this catalyst system.

Calculations

The Catalytic Cycle. The cycle shown in Scheme 1 has been explored previously by use of DFT methods, but different methods and basis sets were employed and the isotope effects were not predicted.[28,57,59] We present here the results of our calculation of the geometries and energies of the species using the mPW1PW91 functional in combination with the SDD basis set for Ru and the triple-ζ basis set 6-311++G** functional for H, N, C, and P. The results match well the experimentally determined geometries of analogous complexes where available, and the activation barrier for the catalytic reaction and the kinetic isotope value.

The cycle begins with the amido, **B**, which reacts with dihydrogen to form an η^2-dihydrogen complex, **C**. The calculated structures of **B** and **C** are shown in Figure 4. The amido bond in **B** between Ru and N1 is notably shorter (1.97 Å) than the Ru−N2 amino bond (2.17 Å). Further evidence of Ru−N1 multiple bond character is that N1 is essentially planar since the sum of the angles around N1 ($\theta_{Ru-N1-H4} + \theta_{H4-N1-C1} + \theta_{C1-N1-Ru} = 355.2°$) is nearly 360°. This shows that N1 is sp^2 hybridized which would allow the free lone pair to donate into an empty d orbital on the Ru. Also of note is the basicity of N1, as evidenced by the APT charge of −0.51 ESU (cf. APT of −0.27 ESU on amino N2). The incoming dihydrogen can coordinate to the vacant site on Ru *trans* to H3. The H1−H2 distance in **C** is 0.81 Å, indicating that the dihydrogen is not very activated at this stage. The Ru−H1 and Ru−H2 distances are nearly identical: 1.84 and 1.83 Å, respectively. The η^2-H_2 ligand is coordinated in such a way as to orient itself parallel to the Ru−N1 bond with H1 closer to N1. The coordination of the H_2 in **C** also results in the loss of multiple bond character between Ru and N1. The Ru−N1 bond distance is elongated to 2.11 Å and the sum of the angles around N1 is far from planar, which would be expected for an sp^3 hybridized nitrogen ($\theta_{Ru-N1-H4} + \theta_{H4-N1-C1} + \theta_{C1-N1-Ru} = 328.9°$). Thus, the calculated structure of **C** is consistent with the cartoon shown in Scheme 1, in which the dative π-bond from the amido group is lost and the lone pair has been pushed back onto the nitrogen. Compared to free H_2 or D_2 and **B**, the relative energy of **C** increases to 7.78 kcal/mol for H_2 and 7.33 kcal/mol for D_2, in the gas phase (Figure 5). Deuterium equilibrium isotope effects have been studied for the reversible addition of H_2 and D_2 to a number of complexes in solution, and it was found that deuterium binds more strongly than does dihydrogen.[38,60]

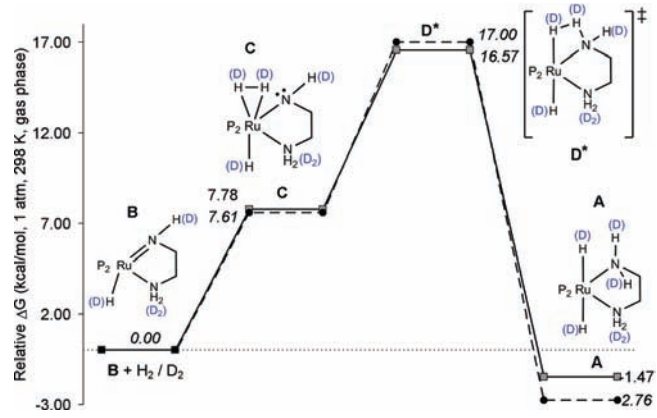

Figure 5. Reaction coordinate diagram for the heterolytic splitting of H_2 (gray squares) or D_2 gas (black circles, energies shown in italics). The reaction starts with **B** + H_2 or D_2, followed by formation of an η^2-dihydrogen/η^2-dideuterium adduct, **C**. This leads to the transition state, **D***, followed by formation of the *trans*-dihydride/*trans*-dideuteride **A**. Energies are reported relative to free **B** and free H_2 or D_2.

The dihydrogen adduct **C** leads directly to the transition state **D*** for the heterolytic splitting of H_2 (Figure 6). In the transition state, the H1−H2 distance has increased from 0.81 in **C** to 1.00 Å in **D***. The magnitude of the negative charge on N1 has also increased from −0.52 to −0.62 ESU. The dihydrogen is now polarized, with H1 assuming a positive charge of 0.44 ESU, and H2, a negative charge of −0.20 ESU. The transition-state motion associated with the imaginary frequency (1172i cm^{-1}) involves the simultaneous lengthening of the H1−H2 bond and the pyramidalization of N1. There is also evidence of the *trans*-influence that H2 has on H3 as the Ru−H3 bond forms since the Ru−H3 bond elongates from 1.63 in **D*** to 1.7 Å in **A**. The structure of **D*** with an H1−H2 distance of 1.00 Å can be considered as a completely unstable elongated dihydrogen complex.[60−64] Furthermore, no bond has yet been formed between N1 and H1, as indicated by the N1−H1 distance of 1.42 Å.

(57) Hedberg, C.; Källström, K.; Arvidsson, P. I.; Brandt, P.; Andersson, P. G. *J. Am. Chem. Soc.* **2005**, *127*, 15083–15090.
(58) Hamilton, R. J.; Bergens, S. H. *J. Am. Chem. Soc.* **2008**, *130*, 11979–11987.
(59) Chen, Y.; Tang, Y.; Lei, M. *Dalton Trans.* **2009**, 2359–2364.
(60) Kubas, G. J. *Metal Dihydrogen and Sigma-Bond Complexes*; Kluwer Academic/Plenum: New York, 2001.
(61) Kubas, G. J. *Chem. Rev.* **2007**, *107*, 4152–4205.
(62) Albinati, A.; et al. *J. Am. Chem. Soc.* **1993**, *115*, 7300−7312.
(63) Hasegawa, T.; Li, Z.; Parkin, S.; Hope, H.; McMullan, R. K.; Koetzle, T. F.; Taube, H. *J. Am. Chem. Soc.* **1994**, *116*, 4352–4356.
(64) Klooster, W. T.; Koetzle, T. F.; Jia, G.; Fong, T. P.; Morris, R. H.; Albinati, A. *J. Am. Chem. Soc.* **1994**, *116*, 7677–7681.

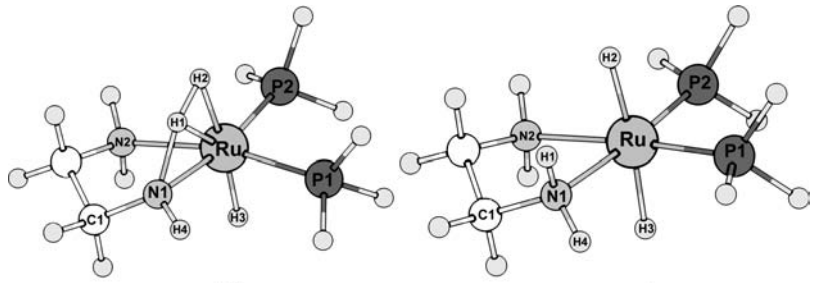

Figure 6. Calculated structures of the models **D*** and **A**. Selected bond lengths (Å) and angles (deg): **D***: Ru−P1 = 2.23, Ru−P2 = 2.25, Ru−N1 = 2.17, Ru−N2 = 2.18, Ru−H3 = 1.63, H1−H2 = 1.01, Ru−H1 = 1.80, Ru−H2 = 1.82, N1−H1 = 1.41, P1−Ru−P2 = 93.4. Selected APT charges (ESU) of **D***: P1 = 1.03, P2 = 1.04, N1 = −0.62, N2 = −0.28, H1 = 0.44, H2 = −0.20, H3 = −0.15.

The relative free energy of **D*** at 298 K, which corresponds to the activation barrier for H_2 heterolytic splitting, is 16.57 kcal/mol for H_2 and 17.00 kcal/mol for D_2. The calculated energy barrier for H_2 agrees fairly well with the experimentally determined activation barrier ($\Delta G^{\ddagger}_{293\ K}$) of 14.5 kcal/mol when using catalyst **1**.[28] For comparison the activation barrier for the dihydride complex **A** transferring dihydrogen to acetone in the six-membered Ru−H−C−O−H−N transition state shown in Scheme 1 is calculated to be only 9.9 kcal/mol (see the Supporting Information). This low-barrier hydrogenation step completes the cycle of Scheme 1.

Hedberg et al.[57] and Chen et al.[59] have also calculated the activation barrier for the cleavage of H_2 based on model complex **B**. Hedberg et al. used single-point energy calculations determined with the B3LYP functional and the triple-ζ basis set LACV3p+** and determined that the activation barrier for H_2 cleavage was 17.2 kcal/mol. This value is also close to the experimentally reported value. Chen et al. used the same functional with the LANL2DZ basis set for ruthenium and 6-31+G** for H, N, C, and P. They calculated the activation barrier for H_2 cleavage to be 22.0 kcal/mol.

The structure following transition state **D*** in Scheme 1 is the *trans*-dihydride **A**. The H1···H2 distance is now 2.54 Å (Figure 6), showing that there is no longer a bond between the two atoms. Of note is that both H1 and H2 are aligned to accommodate an interaction with the polar multiple bond of an incoming substrate such as a carbonyl or imine moiety in a hydrogenation reaction. The charge on the proton H1 is positive, 0.14 ESU, while that on the hydride H2 is negative, −0.22 ESU. This charge distribution would also aid in the orientation of the incoming substrate, since the more electronegative atom of the polar multiple bond (O or N) would preferentially interact with H1, while the electropositive atom (C) would interact with H2. The energy of **A** is −1.47 kcal/mol as a dihydride and −2.76 kcal/mol as a dideuteride relative to the energy of **A** plus H_2 or D_2, indicating that this reaction is thermodynamically favorable.

Calculation of the Kinetic Isotope Effect. This isotope effect was calculated for the system $RuH(NHCH_2CH_2NH_2)(PH_3)_2$ (**B**) plus H_2 versus the partially deuterated catalyst $RuD(NDCH_2CH_2ND_2)(PH_3)_2$ plus D_2 in the gas phase. The $\Delta G_H^{\ddagger}$ value needed for eq 3 above refers to the free energy of the transition state **D*** minus the free energy of **B** plus H_2. Similarly the $\Delta G_D^{\ddagger}$ value refers to the free energy difference for the corresponding deuterated species (Table 3). The calculated KIE effect for the heterolytic splitting of H_2 is 2.1 (Table 3). This value agrees well with that of the measured value for **1** (KIE = 2.0 ± 0.1). Therefore, quantum mechanical tunneling of hydrogen through the barrier to hydrogen splitting does not appear to be important in the catalytic reaction of **1**; otherwise, the experimentally determined KIE would be larger. The magnitude of the experimentally determined KIE suggests an early transition state; that is, the H−H bond is not completely broken, and the structure of **D*** also supports an incomplete cleavage of H_2 in the transition state.

Table 3. Isotope Effects Calculated for the Heterolytic Splitting of Dihydrogen According to Scheme 1 by Various Isotopomers of the Ruthenium Complex **2**

entry	isotopomer	$\Delta G_{D\ 293\ K}^{\ddagger}$ kcal/mol	$\Delta G_D^{\ddagger} - \Delta G_H^{\ddagger}$	KIE
1	$RuD(NDCH_2CH_2ND_2)(PH_3)_2$	17.00	0.43	2.1
2	$RuH(NHCH_2CH_2NH_2)(PH_3)_2$	16.72	0.15	1.3
3	$RuD(NHCH_2CH_2NH_2)(PH_3)_2$	16.89	0.32	1.7
4	$RuH(NDCH_2CH_2ND_2)(PH_3)_2$	16.96	0.39	1.9
5	$RuD(NDCH_2CH_2ND_2)(PH_3)_2$ + MeOD	10.45	0.53	2.5

The isotope effect was also calculated for the catalyst in progressive states of deuteration (Table 3). The KIE for no deuteration of the catalyst (1.3) is not consistent with the observations. When only the Ru−D bond is present in $RuD(NHCH_2CH_2NH_2)(PH_3)_2$, the KIE increases to 1.7. Deuteration of the ethylene diamine N−H groups only (entry 4) results in an increase in KIE to 1.9. The KIE calculated for the proton-shuttle transition state **II** (Figure 1) involving H_2 and MeOH versus D_2 and MeOD is 2.5 (entry 5). In the latter case the catalyst will be completely deuterated as shown in Table 3. Therefore, the best agreement is the value for entry 1 as discussed.

Comparison with the Results from Noyori and Co-workers. Sandoval et al.[25] reported KIE values that greatly depended on the conditions of the hydrogenation or deuteriation of acetophenone in isopropanol or isopropanol-d_8 catalyzed by the complex *trans*-$RuH(\eta^1\text{-}BH_4)$((*S*)-tolbinap)((*S*,*S*)-dpen) (Table 1). The KIE value of 2 for their system with excess base added (KOtBu) best matched our value of 2.0. The value of 55 for the system in the absence of base (other than the BH_4^- ligand which is, in fact, a base[22]) is not consistent with our result.

Noyori and co-workers reported that the KIE of 2 corresponds to the neutral hydrido-amido complex RuH((*S*)-tolbinap)(dpen-amido) reacting with H_2 either via the four-membered TS I of Figure 1 or the six-membered, proton-shuttle TS II of Figure 1. Our results indicate that the four-membered transition state I is more likely.

The low-temperature observation by NMR of intermediates in isopropanol-d_8 reported by Hamilton and Bergens[58] and our group's observations on the effect of iPrOH and base on the activity of catalyst **1**[28] suggest that the presence of base favors the formation of the amido complex. The resting state of the catalysts in neutral iPrOH are the complexes *trans*-RuH(OiPr)

(diphosphine)(diamine). Our use of benzene, a low dielectric constant solvent, disfavors the formation of cationic species such as the cationic transition state **III** of Figure 1 that are formed by reaction with acidic alcohols. The alcohol in our study is the product, 1-phenylethanol, which is a much weaker acid in benzene than is neat isopropanol in the Noyori and Bergens systems.

Conclusions

In summary, the kinetic isotope effect has been determined experimentally to be 2.0 ± 0.1 for the homogeneous hydrogenation of acetophenone catalyzed by *trans*-$RuH_2(NH_2CMe_2CMe_2NH_2)$((*R*)-binap) in benzene under 8 atm of gas (H_2 or D_2) at room temperature. The KIE was also calculated by use of DFT methods to be 2.1 on the basis of the previously proposed mechanism involving the turnover-limiting, heterolytic splitting of dihydrogen or dideuterium across the ruthenium−amido bond of the model complex $RuH(NHCH_2CH_2NH_2)(PH_3)_2$ (**B**) or the deuterated form $RuD(NDCH_2CH_2ND_2)(PH_3)_2$. Thus, the experiment and theory agree well.

The splitting of dihydrogen proceeds via transition state **D*** which has a four-membered Ru···H···H···N ring as proposed earlier.[28] The activation barrier at 298 K calculated using H_2 gas is 16.6 kcal/mol, agreeing reasonably well with the measured value of 14.5 kcal/mol for the activation barrier ($\Delta G^{\ddagger}_{293\ K}$) when using catalyst **1** in the hydrogenation of acetophenone in benzene. For the first time, the activation barrier for D_2 splitting by the deuterated model complex **B** is calculated to be 17.0 kcal/mol.

The predicted KIE value of 2.5 by DFT methods for an alternative mechanism for the catalysis involving the alcohol-assisted splitting of dihydrogen is not consistent with the observed value of 2.0. The value of 2.0 is the same as the isotope effect observed by Sandoval et al. for the hydrogenation/deuteration of acetophenone catalyzed by *trans*-$RuH(\eta^1\text{-}BH_4)$((*S*)-tolbinap)((*S,S*)-dpen) in isopropanol/deuterated isopropanol when KOtBu is added. This might indicate that the transition state for the Noyori system is also the splitting of dihydrogen directly over the ruthenium−amido bond as observed for our catalyst **1**.

Acknowledgment. NSERC is thanked for a Discovery and a Research Tools (reactor) Grant to R.H.M.

Supporting Information Available: Complete refs 43 and 62, a detailed procedure for the catalytic reaction, and coordinates and energies from the DFT calculations including those for the hydrogenation of acetone. This material is available free of charge via the Internet at http://pubs.acs.org.

JA9043104